CONTAMINATION AND FRACTIONATION EFFECTS IN AMS-MEASURED $^{14}C/^{12}C$ AND $^{13}C/^{12}C$ RATIOS OF SMALL SAMPLES

CEES ALDERLIESTEN, KLAAS VAN DER BORG and ARIE F. M. DE JONG

R. J. Van de Graaff Laboratorium, Utrecht University, P.O. Box 80.000, NL-3508 TA Utrecht
The Netherlands

ABSTRACT. In AMS measurements on small ($m \leq 400$ μg) carbon samples, an m-dependence has been noted for the $^{14}C/^{12}C$ and $^{13}C/^{12}C$ ratios that is due to the combined effect of contamination and fractionation. A simple formalism is presented to describe the phenomena and to correct measurements on unknowns for their effect.

INTRODUCTION

For more than ten years the Utrecht AMS facility has been measuring isotopic abundances of cosmogenic radionuclides, primarily of ^{14}C but also of ^{10}Be, ^{26}Al and ^{36}Cl. For ^{14}C, its present state (van der Borg *et al.* 1997) allows a precision of ~0.4% and a detection limit of 2×10^{-15} in routine measurements on recent samples of >0.4 mg of carbon.

Since 1987, *ca.* 6000 ^{14}C samples have been measured for various research projects. One of these projects, ^{14}C dating of the CO_2 enclosed in polar ice (van de Wal *et al.* 1994; van Roijen *et al.* 1995), produced a substantial number of samples with unusually low carbon mass m, typically $m = 35$ μg. It was deemed appropriate to compare such samples with blanks and standards of the same mass and chemical composition, produced in the same graphitization process. From the experience with these and other small samples, two effects emerged (van der Borg *et al.* 1997):

- First, the measured ^{14}C-specific activity of preparation blanks (representing the graphitization process only) increases with decreasing carbon mass. This is as expected and has also been reported by others.
- Second, the measured $^{13}C/^{12}C$ and $^{14}C/^{12}C$ ratios of $m \leq 400$ μg samples of reference material decrease with decreasing mass, and in addition, their mutual relation is "anomalous", *i.e.*, not the quadratic one expected for chemical fractionation processes.

Initially, no explanation for the behavior of the small standards was trusted and its consequences were simply eliminated in the normalization procedure, where the ratios measured for an unknown were combined with those for blanks and standards of the same small mass.

Over the course of years, minor and also major (van der Borg *et al.* 1997) modifications of the setup have been implemented, but the small-standards effects persisted. Meanwhile, mass-dependence was also reported (but not quite believed) by another group with a very different setup (Klinedinst *et al.* 1994). These two facts almost eliminated explanations in terms of AMS effects, such as a sample-dependent emittance/acceptance mismatch. And because fractionation in the Cs sputter source is expected to show a nearly "chemical" behavior (Nadeau *et al.* 1987), the "anomaly" does not seem to originate from AMS as such, so that contamination and fractionation during sample preparation also have to be considered.

AMS SETUP AND SAMPLE PREPARATION

The Utrecht AMS facility has been described previously (van der Borg *et al.* 1997; van der Borg *et al.* 1987). For the present discussion we reiterate that the setup includes a Van de Graaff EN tandem accelerator with a recirculating gas stripper and a high-intensity Cs sputter source (Middleton, Klein

and Fink 1989), and that $^{12,13,14}C$ ions are injected quasi-simultaneously by a fast beam pulser and measured at the high-energy end.

The samples to be discussed here are blanks and standards; the blank CO_2 is obtained by treating IAEA-C1 marble with HCl, the standard CO_2 by combustion of HOxII reference material. Graphite samples of both types (and of the unknowns) are produced by reduction of CO_2 in the presence of H_2 and a catalyst of iron powder (Vogel *et al.* 1984). Large ($m > 1$ mg) samples are made in a 30-cm^3 quartz-Pyrex® unit, small ones in 1/3 of that volume. A computer regulates the oven temperature and monitors the pressure in the graphitization tube. The graphitization process is stopped after *ca.* 3 h, when the pressure has clearly leveled off to a stable value. For $m > 0.2$ mg samples, the mass ratio Fe/C is *ca.* 4.0, but for practical reasons m_{Fe} is not decreased below 0.8 mg, so that Fe/C mass ratios can go up to 40 for the smallest samples. The Fe/C powder is pressed into the $\varnothing = 2.0$ mm hole of an aluminum target holder; for small samples, some silver powder is used as a "sticking" layer on the bottom.

Measurements and Results

The small carbon samples were measured in special batches, with the 22-position sample wheel containing 1) the small unknowns; 2) a disc of commercial graphite, a normal blank and one or two normal standards; and 3) small blanks and standards, more or less covering the mass range of the unknowns. The results to be discussed below are those for the small blanks and standards used over the last two years and include the small-sample data already presented (van der Borg *et al.* 1997). As expected, small samples last a shorter measuring time than normal ones and during this time they yield lower currents (typically starting at *ca.* 60% of the normal value); results for currents below 10% of the normal value are rejected. The results are displayed in Figures 1 and 2 as r^{13} and r^{14}; these are the $^{13}C/^{12}C$ and $^{14}C/^{12}C$ ratios for small samples normalized on the corresponding values for the normal HOxII standard(s) measured in the same batch.

Contamination and Fractionation

The Model

The r^{13} and r^{14} data in Figure 2 show that fractionation as well as contamination plays a role: the narrow $^{13}C/^{12}C$ range in nature excludes the possibility that a reasonable admixture of any contaminant could produce the $r_s^{13}(m)$ data of Figure 2A; on the other hand, given those data, chemical (quadratic) fractionation alone would only partly explain the decrease of $r_s^{14}(m)$ with decreasing mass shown in Figure 2B. However, when fractionation is combined with contamination, of all blanks and standards, with carbon of a $^{14}C/^{12}C$ ratio well below that of the standard material, we get a qualitative explanation of Figures 1 and 2. For this reason the data are compared with a formalism based on the following premises:

1. *Mass-dependent* isotopic fractionation is of the "chemical" type and can occur both during the graphitization (which may become progressively incomplete for smaller and smaller CO_2 samples) and in the negative-ion formation (if this process is, *e.g.*, Fe/C mass-ratio dependent, Arnold *et al.* 1987).
2. All contamination precedes graphitization. In reality this is not true, but in the model it simplifies the formalism, with negligible quantitative inaccuracy at any practical level of contamination.
3. Contamination does not affect the $^{13}C/^{12}C$ ratio (see above).

https://doi.org/10.1017/S0033822200018075 Published online by Cambridge University Press

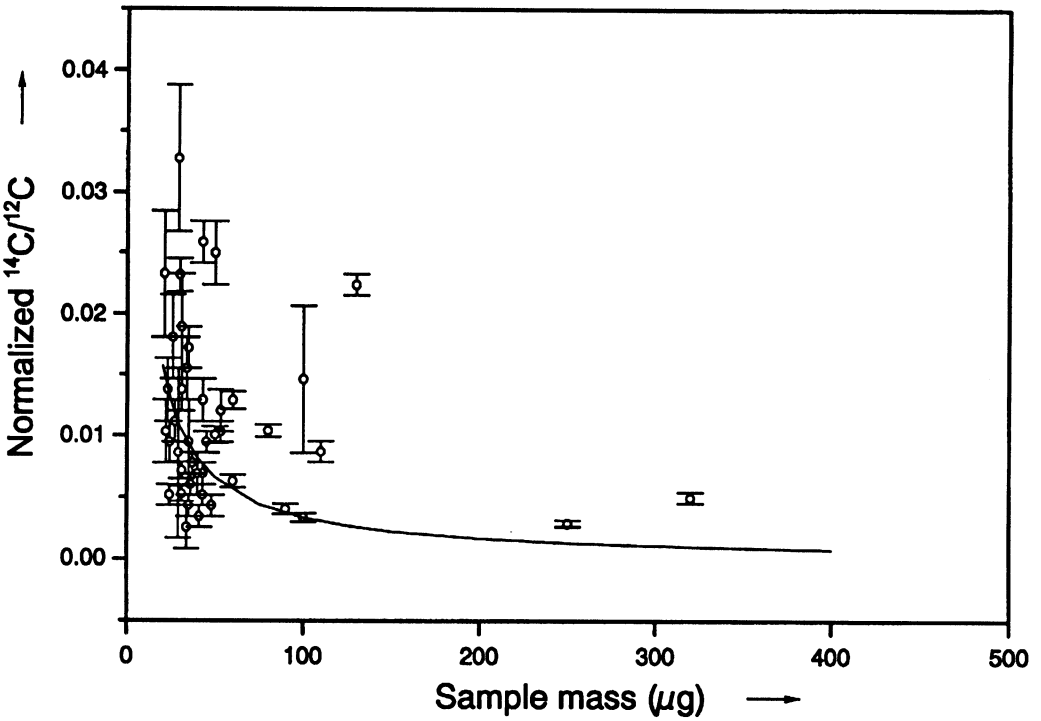

Fig. 1. Normalized AMS-measured $^{14}C/^{12}C$ ratios of small blank samples, plotted against sample carbon mass; for normalization, see text. The curve represents the function $r_b^{14} = f^{14}(m)\beta r_c^{14}$ with the values for f^{14}, β and r_c^{14} derived from the present data.

4. Mass and isotopic composition of the contaminant have a (mean) value that is independent of mass and type (blank, standard, unknown) of the original sample.
5. The original blank is ^{14}C-dead.
6. Only contamination produces background counts.

The unknowns in this model are the mean $^{14}C/^{12}C$ ratio of the contaminant and the mean contaminant mass. The translation of the model into formulas is straightforward (Donahue, Linick and Jull 1990; Brown and Southon 1997); a new aspect is that now both $^{14}C/^{12}C$ and $^{13}C/^{12}C$ are considered, so that fractionation as well as contamination can be taken into account.

The Formulas

The effect of contamination on $R^{14} \equiv {}^{14}C/^{12}C$ and $R^{13} \equiv {}^{13}C/^{12}C$ is well described by the simple *two*-isotopes mixing formula. When a CO_2 standard sample of mass m (contamination included) is graphitized and subsequently measured with AMS, one gets $R_s^{14}{}_{\rm exp}(m) \equiv \alpha_0\alpha^{14}(m)R_s^{14}{}_{\rm mix}$, with $R_s^{14}{}_{\rm mix} = ((m-m_c)R^{14}({\rm Std}) + m_c R_c^{14})/m$ for a small sample, $R_s^{14}{}_{\rm exp}(\infty) = \alpha_0\alpha^{14}(\infty)\, R_s^{14}{}_{\rm mix}(\infty)$ for a "large" one. Here, α_0 stands for sample-mass *independent* fractionation (in, *e.g.*, the stripper), $\alpha^{14}(m)$ for the combined fractionation in graphitization and negative-ion formation and R^{14}(Std) for the original $^{14}C/^{12}C$ ratio of the standard material (in our case HOxII); the subscripts s, b, x and c refer to standard, blank, unknown and contaminant, respectively. Normalization yields

$$r_s^{14}(m) \equiv R_s^{14}{}_{\rm exp}(m)/R_s^{14}{}_{\rm exp}(\infty) = f^{14}(m)(1-\beta+\beta r_c^{14}) \,, \qquad (1)$$

https://doi.org/10.1017/S0033822200018075 Published online by Cambridge University Press

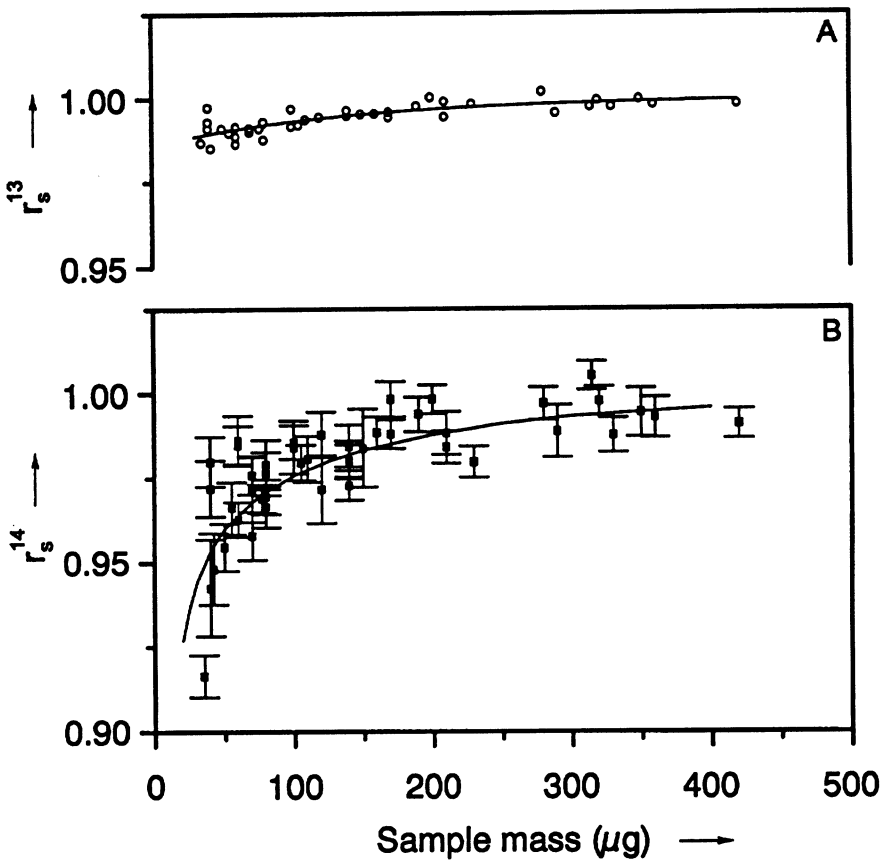

Fig. 2. Normalized AMS-measured isotope ratios of small standard samples, plotted against sample carbon mass; for normalization, see text. A. Normalized $^{13}C/^{12}C$ ratio; the curve represents the least-squares fitted function $r(m) = (1 - a_1 e^{-a_2 m})$ ($a_1 = 0.014$, $a_2 = 0.007$; m in μg) chosen to parametrize the data. B. Normalized $^{14}C/^{12}C$ ratio; the curve represents the model function $r_s^{14} = f^{14}(m)(1 - \beta + \beta r_c^{14})$ with the values for f^{14}, β and r_c^{14} derived from the present data.

where $f^{14}(m) \equiv \alpha^{14}(m)/\alpha^{14}(\infty)$ denotes the fractionation factor normalized to that of "large" samples, $\beta \equiv m_c/m$ the relative amount of contaminant carbon, and $r_c^{14} \equiv R_c^{14}/R_{mix}^{14}(\infty) \equiv R_c^{14}/R^{14}(\text{Std})$. Along similar lines, one finds

$$r_b^{14}(m) = f^{14}(m)\beta r_c^{14} \tag{2}$$

for a contaminated blank and for $^{13}C/^{12}C$ ratios, using assumption number 3 above,

$$f^{13}(m) = r^{13}(m) \ . \tag{3}$$

With $f^{13}(m)$ from experiment and $f^{14}(m) = (f^{13}(m))^2$, the unknowns β and r_c^{14} can be resolved from Equations 1 and 2:

$$\beta = 1 + (r_b^{14}(m) - r_s^{14}(m))/f^{14}(m) \tag{4}$$

and

$$r_c^{14} = r_b^{14}(m)/(f^{14}(m) + r_b^{14}(m) - r_s^{14}(m)) \ , \tag{5}$$

https://doi.org/10.1017/S0033822200018075 Published online by Cambridge University Press

from which $m_c = \beta m$ and $R_c^{14} = r_c^{14} R^{14}(\text{Std})$ can be calculated for values of m at which measured or interpolated $r_s^{14}(m)$ and $r_b^{14}(m)$ data are available. These m_c and R_c^{14} values (and their errors) can then be used in a normalization formula valid for both small and normal unknowns (assuming, as before, type-independent contamination). For the present model this formula reads:

$$\frac{R_x^{14}}{R^{14}(\text{Std})} = \frac{Q}{f^{14}(m_x)(1-\beta_x)}\{f^{14}(m_s)(1-\beta_s+\beta_s r_c^{14}) - f^{14}(m_b)\beta_b r_c^{14}\} + \frac{f^{14}(m_b)}{f^{14}(m_x)}\frac{\beta_b r_c^{14}}{(1-\beta_x)} - \frac{\beta_x r_c^{14}}{(1-\beta_x)}, \tag{6}$$

where $Q \equiv (R_{x\,\text{exp}}^{14} - R_{b\,\text{exp}}^{14})/(R_{s\,\text{exp}}^{14} - R_{b\,\text{exp}}^{14})$ contains all the experimental results for unknown, standard and blank and the function $f^{14}(m)$ their mass-dependent fractionation. The quantities m_c and r_c^{14}, characterizing the (mean) contamination, are deduced from separate measurements on small blank and standard samples, as discussed above; they are valid as long as preparation and measuring conditions are not changed.

In Equation 6, all sample masses are assumed to be "finite", but the blanks and standards used in practice are usually "large enough", which implies (β_s, $\beta_b \to 0$; $f^{14}(m_s)$, $f^{14}(m_b) \to f^{14}(\infty) = 1$) and reduction of Equation 6 to

$$\frac{R_x^{14}}{R^{14}(\text{Std})} = \frac{Q}{f^{14}(m_x)(1-\beta_x)} - \frac{\beta_x r_c^{14}}{(1-\beta_x)}. \tag{7}$$

This is the more practical formula in the present model to normalize unknowns of any mass m_x. Note that if these unknowns are also large, then ($\beta_x \to 0$; $f^{14}(m_x) \to f^{14}(\infty) = 1$), and Equation 7 reduces to the simple and much-used expression $R_x^{14} = QR^{14}(\text{Std}) = \{(R_{x\,\text{exp}}^{14} - R_{b\,\text{exp}}^{14}) / (R_{s\,\text{exp}}^{14} - R_{b\,\text{exp}}^{14})\} R^{14}(\text{Std})$.

Discussion

The above formalism has been applied to the data given in Figures 1 and 2. Functions of the type $r(m) = 1 - a_1 e^{-a_2 m}$ have been least-squares fitted to parametrize the r_s^{14} (m) and r_s^{13} (m) data sets; from the latter one extracts the function $f^{13}(m)$ (see Equation 3) and thus the function $f^{14}(m)$.

The expression $r(m) = a + b/m$ is least-squares fitted to the r_b^{14} values. These have a large spread (see Fig. 1) that tends to obscure the systematic mass-dependence of the mean. This reflects the partly random character of the contamination process, which becomes clearer for smaller samples. For larger blanks, the mean contamination does not go to zero with $1/m$ as implied in the model, but rather to some finite value somewhat below 0.15 percent of Modern Carbon (pMC), the mean level for ~1-mg preparation blanks. Even the background measured on massive graphite discs (no chemistry) is not zero but ~0.05 pMC. The fact that both background levels tend to decrease with increasing beam current is a further indication of an additional ^{14}C background component, not strictly proportional to the ^{12}C beam intensity and therefore probably derived from cross-contamination in the ion source. Ions wrongly identified as ^{14}C, however, are certainly of minor importance.

The parametrizations of $f^{14}(m)$, $r_s^{14}(m)$ and $r_b^{14}(m)$ provide the input for Equations 4 and 5 to calculate m_c and R_c^{14} for m-values in the small-sample mass range. We find $m_c = 1.4 \pm 0.5$ µg and $R_c^{14} = 33 \pm 11$ pMC. With these values, Equations 1 and 2 provide the $r_s^{14}(m)$ and $r_b^{14}(m)$ curves shown in Figures 1 and 2. We conclude that the mass-dependence is reproduced by a combination of chemical

https://doi.org/10.1017/S0033822200018075 Published online by Cambridge University Press

fractionation and mass-independent contamination, with "reasonable" results for mass and specific ^{14}C activity of the contaminant: the m_c value is a small but non-negligible fraction of the smallest sample masses and the R_c^{14} value is well below that of contemporary material.

Formulas to describe the effect of contamination in ^{14}C measurements on small samples have been derived and confirmed by Brown and Southon (1997). Their model shares with ours the assumption that an admixture of a contaminant with constant mass and specific activity is present in blanks, standards and unknowns. But their AMS measurements were restricted to $^{14}C/^{13}C$ ratios and consequently cannot detect a possible mass-dependence of fractionation effects (assumed by Brown and Southon (1997) to be at most secondary) in preparation and/or measurement. We can only report that *our* data for $m < 400$ μg reveal mass-dependent fractionation.

For our smallest samples, fractionation originates largely from the *graphitization:* although the process is continued until an unambiguous leveling of the pressure curve shows that the conversion of CO_2 should be complete, nevertheless recombustion and subsequent mass-spectrometric analysis of small graphite samples (van der Borg *et al.* 1997) have demonstrated that $^{13}C/^{12}C$ fractionation (compared to that for large samples) increases by up to 2% when m decreases to 25 μg—in agreement with the results from AMS $^{13}C/^{12}C$ measurements on similar samples. A smaller part is expected from the fractionation in the C^- ion formation, where *Fe/C mass-ratio dependence* has been observed in an experiment by Arnold *et al.* (1987). They reported a ~1% increase of the fractionation when the Fe/C ratio increases from 7 to 25. Although the absence of fractionation in the graphitization was not proven, their test samples were relatively large ($m > 200$ μg), so we assume that indeed a Fe/C dependence rather than fractionating graphitization has been demonstrated.

The applicability of the model to the present data set does *not* depend on any assumption about the relative contributions of the two mechanisms just mentioned: for $m < 200$ μg, the amount of Fe is constant, so data are specified by m alone and can be fitted with an empirical function $f_<^{13}(m)$, whereas for $m > 200$ μg, the Fe/C mass ratio is fixed, only m as such labels the data and an empirical function $f_>^{13}(m)$ can be determined. For the present $^{13}C/^{12}C$ values no difference in $f^{13}(m)$-behavior can be observed, so one parametrization was enough for the whole sample-mass range (see Fig. 2A). The function(s) $f^{13}(m)$ thus obtained can be applied as long as the fractionations of ^{13}C and ^{14}C have a known relation (taken as quadratic in the present model) for the processes involved.

As for the parameters reported by Brown and Southon (1997) to account for their test data, these are in notable agreement with ours: $m_c = 2.6$ μg *vs.* $m_c = 1.4$ μg and $R_c^{14} = 44$ pMC *vs.* $R_c^{14} = 33$ pMC. As the deduction of our values includes correction for fractionation, we repeated it with $f^{14} = 1$ and found $m_c = 2.6$ μg and $R_c^{14} = 20$ pMC. Such an agreement must be considered as fortuitous, but the general picture may suggest a common "mechanism" of contamination in both laboratories. A similar remark can be made about the observed less-than-$(1/m)$ decrease of the ^{14}C content of preparation blanks.

Conclusion

In AMS measurements on small ($m \leq 400$ μg) carbon samples, a systematic sample-mass dependence of the measured isotope ratios may occur; at the Utrecht AMS facility, $^{14}C/^{12}C$ deficits of >5% have been observed. The effects are explained as due to a combination of 1) a sample-mass *independent* contamination during sample preparation and 2) a sample-mass *dependent* fractionation, presumably in both graphitization and negative-ion formation. AMS measurements of not only $^{14}C/^{12}C$ but also $^{13}C/^{12}C$ ratios allow a separation of the two factors. In the model description of the mass-dependences, the (mean) mass and ^{14}C concentration of the contaminating carbon are fitted as

https://doi.org/10.1017/S0033822200018075 Published online by Cambridge University Press

free parameters and get reasonable values. A formula is derived in which these values are used to account for all small-sample effects. This provides a "unified" background-subtraction/normalization procedure for both small and large samples.

References

Arnold, M., Bard, E., Maurice, P. and Duplessy, J.-C. 1987 ^{14}C dating with the Gif-sur-Yvette tandetron accelerator: Status report. *Nuclear Instruments and Methods in Physics Research* B29: 120–123.

Brown, T. A. and Southon, J. R. 1997 Corrections for contamination background in AMS ^{14}C measurements. *Nuclear Instruments and Methods in Physics Research* B123: 208–213.

Donahue, D. J., Linick, T. W. and Jull, A. J. T. 1990 Isotope-ratio and background corrections for accelerator mass spectrometry radiocarbon measurements. *Radiocarbon* 32(2): 135–142.

Klinedinst, D. B., McNichol, A. P., Currie, L. A., Schneider, R. J., Klouda, G. A., von Reden, K. F., Verkouteren, R. M. and Jones, G. A. 1994 Comparative study of Fe-C bead and graphite target performance with the National Ocean Science AMS (NOSAMS) facility recombinator ion source. *Nuclear Instruments and Methods in Physics Research* B92: 166–171.

Middleton, R., Klein, J. and Fink, D. 1989 A CO_2 negative ion source for ^{14}C dating. *Nuclear Instruments and Methods in Physics Research* B43: 231–239.

Nadeau, M.-J., Kieser, W. E., Beukens, R. P. and Litherland, A. E. 1987 Quantum Mechanical effects on sputter source isotope fractionation. *Nuclear Instruments and Methods in Physics Research* B29: 83–86.

van der Borg, K., Alderliesten, C., de Jong, A. F. M., van den Brink, A., de Haas, A. P., Kersemaekers, H. J. H. and Raaymakers, J. E. M. J. 1997 Precision and mass fractionation in ^{14}C analysis with AMS. *In* Jull, A. J. T., Beck, J. W., and Burr, G. S., eds., Proceedings of the 7th International Symposium on Accelerator Mass Spectrometry. *Nuclear Instruments and Methods in Physics Research* B123: 97–101.

van der Borg, K., Alderliesten, C., Houston, C. M., de Jong, A. F. M. and van Zwol, N. A. 1987 Accelerator mass spectrometry with ^{14}C and ^{10}Be in Utrecht. *Nuclear Instruments and Methods in Physics Research* B29: 143–145.

van de Wal, R. S. W., van Roijen, J. J., Raynaud, D., van der Borg, K., de Jong, A. F. M., Oerlemans, J., Lipenkov, V. and Huybrechts, P. 1994 From $^{14}C/^{12}C$ measurements towards radiocarbon dating of ice. *Tellus* 46(B): 94–102.

van Roijen, J. J., van der Borg, K., de Jong, A. F. M. and Oerlemans, J. 1995 Ages and ablation and accumulation rates from ^{14}C measurements on antarctic ice. *Annals of Glaciology* 21: 139–143.

Vogel, J. S., Southon, J. R., Nelson, D. E. and Brown, T. A. 1984 Performance of catalytically condensed carbon for use in accelerator mass spectrometry. *Nuclear Instruments and Methods in Physics Research* B5: 289–293.